THE ROYAL SOCIETY

Neuronal population activity and functional imaging

Jack W. Scannell* **and Malcolm P. Young**

Department of Psychology, University of Newcastle, Newcastle-upon-Tyne NE1 7RU, UK

Human functional brain imaging detects blood flow changes that are thought to reflect the activity of neuronal populations and, thus, the responses of neurons that carry behaviourally relevant information. Since this relationship is poorly understood, we explored the link between the activity of single neurons and their neuronal population. The functional imaging results were in good agreement with levels of population activation predicted from the known effects of sensory stimulation, learning and attention on single cortical neurons. However, the nature of the relationship between population activation and single neuron firing was very surprising. Population activation was strongly influenced by those neurons firing at low rates and so was very sensitive to the baseline or 'spontaneous' firing rate. When neural representations were sparse and neurons were tuned to several stimulus dimensions, population activation was hardly influenced by the few neurons whose firing was most strongly modulated by the task or stimulus. Measures of population activation could miss changes in information processing given simultaneous changes in neurons' baseline firing, response modulation or tuning width. Factors that can modulate baseline firing, such as attention, may have a particularly large influence on population activation. The results have implications for the interpretation of functional imaging signals and for cross-calibration between different methods for measuring neuronal activity.

Keywords: fMRI; PET; MT; V5; Vl; inferotemporal cortex

1. INTRODUCTION

Human functional imaging explores the brain by correlating local blood flow with particular tasks, stimuli or behavioural states (Petersen *et al*. 1988; Tootell *et al*. 1995; Frith & Friston 1997). The small blood flow changes that imaging detects are important because they are presumed to follow from changes in the activity of the populations of neurons responsible for the functions in question (Petersen *et al*. 1988; Tootell *et al*. 1995; Malonek & Grinvald 1996; Frith & Friston 1997). However, the links between the behaviourally relevant information carried by neurons (Georgopoulos *et al*. 1986; Newsome *et al*. 1989; Britten *et al*. 1992), total activity in the neuronal population, neuronal metabolic rate and changes in local cerebral blood flow are unclear (Boynton *et al*. 1996; Malonek & Grinvald 1996; Poeppel 1996; Friston 1997; Poirson *et al*. 1997). This paper explores one of these links, the relationship between the response properties of single neurons and summed activity in the neuronal population.

Formal models have clarified the relationship between cellular- and ensemble-level behaviour in a number of areas of neuroscience (e.g. Knight 1972; Kristan & Shaw 1997). We believe that similar formalization is necessary to help clarify the relationship between single cell and population activity. First, from the tuning properties of cortical neurons, we were not sure whether some stimuli that give increased haemodynamic signals in functional imaging experiments will necessarily cause a net increase in the activity of the neuronal population. Second, several aspects of neuronal tuning, including peak firing rate, tuning width and baseline firing rate, vary with task and stimulus. It is not clear how these will interact to influence population activation. This is illustrated with data recorded from neurons in cortical area MT (data provided by W. Newsome) while awake behaving macaques performed a motion discrimination task (Newsome *et al*. 1989; Britten *et al*. 1992). The data provide an example of an interaction between peak and baseline firing, which could make a functional change invisible to measures of population activity. Third, we were surprised by the small effect of visual stimulation on the mean firing rate of visually responsive neurons recorded in the inferotemporal (IT) cortex of awake macaques (Baddeley *et al*. 1997). When animals viewed a blank screen the mean firing rate was 14 Hz, which increased to only 18 Hz when the animals viewed films. This effect is modest and is comparable with shifts in the mean firing rate that are caused by attentional changes without any change in sensory stimulation in some cortical areas (e.g. Treue & Maunsell 1996). In the absence of visual stimulation, increased attention raises the mean firing rate of neurons in macaque area V4 from 10 to 13 Hz (Luck *et al*. 1997).

The rest of this paper considers first, the relationship between the mean local neuronal firing rate and imaging signals; second, real electrophysiological data to highlight possible problems in interpreting imaging signals; and third, a formal model to explore the relationship between the behaviour of neurons and the activity of the population that they compose.

*Author for correspondence (j.w.scannell@ncl.ac.uk).

Received 2 November 1998 *Accepted* 26 January 1999

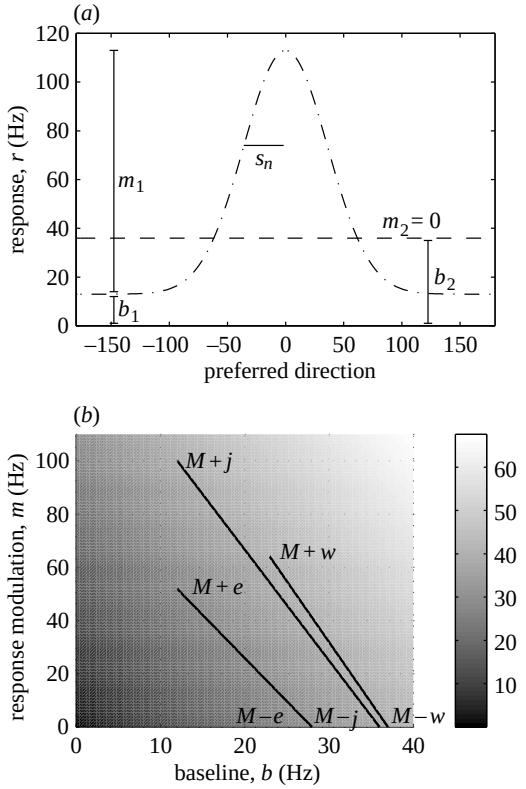

Figure 1. (*a*) Neuronal responses across an MT direction hypercolumn. The dotted and dashed line shows the mean firing rates of MT neurons with different direction preferences to a strong motion signal, a 100% coherent random dot kinetogram moving at 0° (Newsome *et al*. 1989; Britten *et al*. 1992). Parameter b_1 is the baseline firing rate, m_1 is the degree of response modulation and s_n is the standard deviation of neuronal direction tuning. We estimated the mean firing rate to coherent motion across the hypercolumn by fitting a Gaussian tuning curve with a peak of $b_1 + m_1$, a minimum of b_1 and standard deviation s_n, using a mean tuning bandwidth for MT neurons of 84° (Albright 1984). The dashed line shows the mean firing rates of neurons to an equivalent stimulus with no overall direction of motion, a 0% coherent random dot kinetogram. Here, b_2 is the baseline firing rate and m_2, the degree of response modulation, is zero. For this stimulus condition, the mean firing rate across the hypercolumn was simply b_2. The areas under the dashed and the dotted and dashed lines are similar, indicating a similar mean firing rate across the hypercolumn in the two conditions. (*b*) The mean firing rate across the MT population can remain constant despite marked changes in information processing. The grey scale represents the mean firing rate (in Hz) across the hypercolumn and was computed from the Gaussian neuronal response curve. The axes show the mean response modulation *m* (*y*-axis) and mean baseline firing rate *b* (*x*-axis). Parameters *m* and *b* were the mean peak and baseline firing rates of large numbers of single neurons recorded in area MT in three animals under the same two stimulus conditions outlined in (*a*); 100% coherent kinetograms (M +) and 0% coherent kinetograms (M −). For each individual animal (*e*, *j* and *w*), the lines link points showing the response modulation *m*, baseline firing rate *b* and mean firing rate within the hypercolumn in the M + and M − stimulus conditions. Although MT neurons show unambiguous directional responses in the M + condition and no directional tuning in the M − condition, there is either a very slight reduction (animal *e*) or a very slight increase (animal *j*) in the mean population firing rate from M + to M − . This is because the reduction in response modulation is balanced by an increase in baseline.

2. METHODS AND RESULTS

(a) *Population activity and functional imaging signals*

In common with other recent work (Tagamets & Horwitz 1998), we suppose a linear relationship between the magnitude of the imaging signal and the number of spikes fired in the local neuronal population within the volumes that are resolved in most human imaging experiments (Grinvald *et al*. 1994; Malonek & Grinvald 1996; Engel *et al*. 1997). We think that this simple approach agrees with widely held assumptions in functional imaging (Boynton *et al*. 1996; Tagamets & Horvitz 1998). First, most of the metabolic cost of neural transmission is incurred at synapses (Yarowsky *et al*. 1983). Second, there is an approximately linear relationship between the firing rate of neurons and metabolic activity at their synapses (Kadekaro *et al*. 1987). Third, approximately 90% of synapses in the cortex are local. The vast majority of both excitatory and inhibitory nerve terminals in any cortical area originate in nearby cells (Peters *et al*. 1994; Douglas *et al*. 1995; Somers *et al*. 1995). Therefore, the metabolic cost of synaptic activity is usually the consequence of a spike in a nearby neuron. Fourth, extrinsic thalamocortical and corticocortical connections are excitatory (Crick & Asamuma 1986). Fifth, both empirical and theoretical studies suggest that cortical neurons exist in a 'high-input regime' with a local balance between excitatory and inhibitory neuronal activity (e.g. Somers *et al*. 1995; Shadlen & Newsome 1998; Tagamets & Horvitz 1998; Van Vreeswijk & Sompolinsky 1998). Strong intrinsic connections mean that substantial mismatches between extrinsic drive and intrinsic activity are short lived, local excitatory and inhibitory populations closely track each others' activity and the population response to extrinsic drive is linearized (Shadlen & Newsome 1998; Tagamets & Horwitz 1998; Van Vreeswijk & Sompolinsky 1998). Therefore, it is unlikely that a substantial volume of cortex could sustain a high level of inhibitory activity, producing a simultaneously low spiking rate and high metabolic rate (Raichle 1998), although this may occur to a limited extent at the level of the cortical column (Somers *et al*. 1995). For these reasons, we expect the sum of spikes in the population to be closely reflected in local synaptic activity (Arieli *et al*. 1995, 1996) and metabolic rate (Yarowsky *et al*. 1983).

(b) *Population activity in area MT*

Area MT neurons are highly selective to the direction of motion within their receptive fields (Zeki 1974; Albright 1984) and carry behaviourally important motion signals (Newsome *et al*. 1989; Britten *et al*. 1992). To examine the effect of motion signals on the mean firing rate in a population of MT (data from W. Newsome) neurons, we used single neuron data that were recorded in awake monkeys that judged the direction of motion of attended random dot kinetograms. The population corresponded to a direction hypercolumn, a local area of cortex across which all preferred directions of motion are represented once. These data provide a direct example of a major functional change that had very little effect on the mean firing rate of a neuronal population.

The mean firing rate in the hypercolumn was calculated from the firing rates of a large number of neurons recorded in two stimulus conditions in three different animals (see the caption to figure 1). In the first condition, neurons were shown patterns of coherently drifting dots, a strong visual motion stimulus, moving either in their preferred direction or at 180° to it. The mean firing rate across the hypercolumn was then

computed from the known tuning properties of MT neurons (Albright 1984). In the second condition, neurons were shown dynamic twinkling dots, which lack coherent motion (figure 1*a*). Figure 1*b* shows that a reduction in response modulation between the coherent motion (M+) and non-coherent motion (M−) conditions may be balanced by an increase in the baseline firing rate. This shows how an unequivocal difference in information processing in a neuronal population can be accompanied by small and individually variable differences in the mean firing rate. In fact, this analysis is likely to underestimate the effect of baseline shifts (see below) and overestimate the effect of changes in response modulation as it assumes MT neurons are tuned to a single stimulus dimension, direction of motion. In this case, stimulus speed and location were also adjusted to suit each neuron (Britten *et al*. 1992).

(c) *Model of population activity and single neuron tuning*

We extended the reasoning applied to electrophysiological data from area MT to explore systematically the relationship between the response properties of single neurons, the total number of spikes fired by neurons in the population and the magnitude of the imaging signal. Our model (described in detail below) was as simple as was consistent with an excellent fit of the experimental data. Five parameters represent the activity of the single neurons: d is the number of stimulus dimensions to which neurons are tuned, x is the single neurons' preferred stimulus vector, s_n is the single neuron tuning width relative to the range of neuronal preferences in the population that generates the imaging signal, m is the difference in neuronal response probability between best and worst stimulus and b is the baseline neuronal response probability (figure 1*a*).

These parameters capture major aspects of single neuron tuning. Real neurons are tuned to several stimulus dimensions, including azimuth, elevation, orientation and direction and speed of motion in the case of MT (Albright 1984). Real neuronal preferences vary across the population and can change substantially with attention (Maunsell & Ferrera 1995; Connor *et al*. 1997) and learning (Miyashita 1988; Sakai & Miyashita 1991; Sobotka & Ringo 1993). The stimulus-dependent modulation of single neuron firing (m) can vary with stimulus intensity (e.g. contrast of visual stimuli), stimulus characteristics (Albright 1984), attention (Motter 1993, 1994; Treue & Maunsell 1996; Connor *et al*. 1997; Luck *et al*. 1997) and, possibly, learning (Miyashita 1988; Sakai & Miyashita 1991; Fahy *et al*. 1993; Sobotka & Ringo 1993). The neuronal tuning width relative to the range of preferences of neurons contributing to the imaging signal (s_n) can vary with stimulus characteristics (Albright 1984), learning (Miyashita 1988; Sakai & Miyashita 1991; Sobotka & Ringo 1993) and imaging method. Baseline firing (b) is very sensitive to attention in some cortical areas (Treue & Maunsell 1996; Luck *et al*. 1997), can vary with stimulus type (Albright 1984; Newsome *et al*. 1989; Britten *et al*. 1992) and may be modulated by other factors such as arousal, cognitive load or learning.

Our model consists of a large population of neurons within a voxel of cortex. The population's instantaneous neuroimaging signal is the sum of activity of all the neurons in the voxel, given by A,

$$A = \int p(r)\mathrm{d}V. \tag{1}$$

Here, $p(r)$ is the instantaneous probability of a spike per neuron (proportional to the mean firing rate in the population) and the integral is over all neurons in the imaging voxel. The discharge probability $p(r)$ can be expressed in terms of the response probability ($p(r|x)$) of a neuron firing a spike given that the neuron's optimum stimulus is x and the probability $p(x)$ that a neuron sampled at random in the voxel has an optimum stimulus of x (figure 2*a*,*b*),

$$p(r) = \int p(r|x)p(x)\mathrm{d}x. \tag{2}$$

The term $p(r)$ is calculated by integrating over all stimulus preferences (the area under the solid line in figure 2*c*). The first term of the integral, $p(r|x)$, corresponds to the neurons' receptive field (figure 2*a*). In our model, this is characterized by a multivariate Gaussian distribution with standard deviation s_n, where x_s is the presented stimulus itself (figure 2*a*),

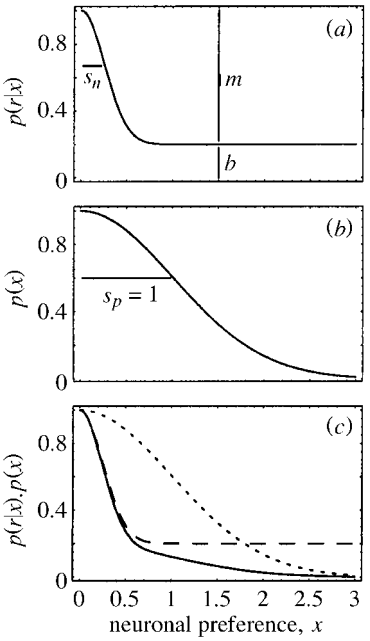

Figure 2. The activation model. In the example here, cells are tuned to a single stimulus dimension within a voxel in which neuronal preferences are centred on the presented stimulus, $x_p = x_s = 0$. (*a*) The single neuron response probability $p(r|x)$ varies with the neuronal preference x. Parameter s_n, in this case 0.25, is the standard deviation of the neuronal tuning curve, b represents the neurons' baseline response probability and m represents the difference in response probability between most and least active neurons (equation (3)). (*b*) $p(x)$, the relative frequency of neurons with different preferences within the voxel (equation (4)). The standard deviation of neuronal preferences within the voxel is s_p, which we set to one. The single unit tuning s_n, is thus the ratio of the tuning width of single cells to the range of preferences within the voxel. For most of our analyses $s_n = 0.25$, so s_p can be regarded as less than one direction hypercolumn in area MT (Albright 1984) or less than one orientation hypercolumn in area V1 (Somers *et al*. 1995). This ratio of single neuron tuning width to voxel size is higher than is resolved in most human functional imaging experiments, but is lower than the resolution of mapping signals in optical imaging. (*c*) The solid line shows $p(r|x)p(x)$, the contribution of different components of the population to $p(r)$, the instantaneous probability of a spike per neuron, which corresponds to the area under the solid line (equation (2)). Here, $p(r|x)p(x)$ is the product of the single neuron response probability $p(r|x)$ (dashed line) and the relative frequency of single neurons with different preferences $p(x)$ (dotted line) within the voxel.

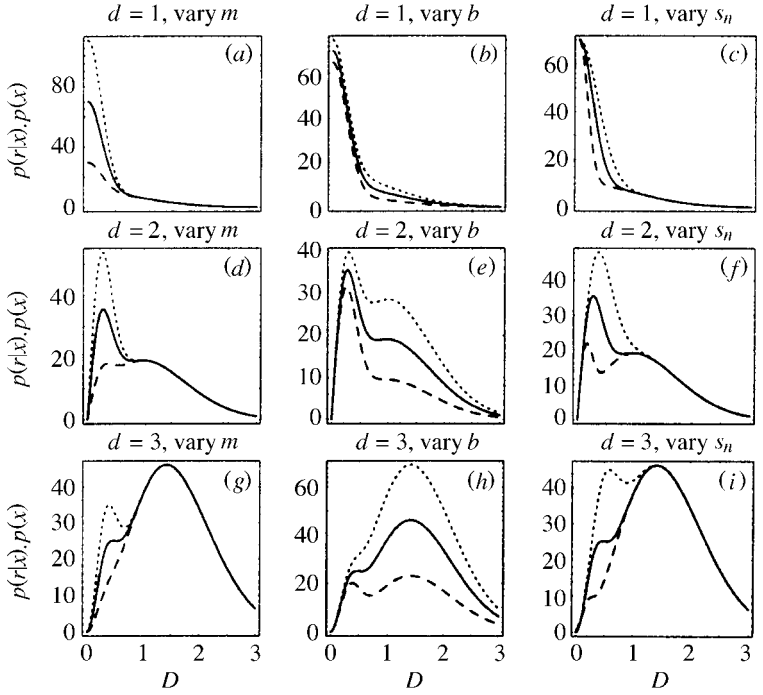

Figure 3. Variations in response modulation, baseline firing and neuronal tuning width influence the imaging signal. The vertical axis represents $p(r|x)p(x)$, the contribution of different components of the population to $p(r)$, the instantaneous neuronal response probability. Both $p(r)$ and the imaging signal A are proportional to the area under each curve. The horizontal axis represents D, the absolute difference between neuronal preference and both the central preference of the voxel and the presented stimulus (see text). The effects of response modulation, baseline firing and neuronal tuning width depend strongly on the number of stimulus dimensions to which neurons are tuned. The top, middle and bottom rows of plots show populations tuned to $d=1$, $d=2$ and $d=3$ stimulus dimensions. The solid line is comparable across all plots and was computed with response modulation $m=60$ Hz, baseline $b=10$ Hz and tuning width $s_n=0.25$. In all plots, $b=10$ Hz, $m=60$ Hz and $t=0.25$ unless stated otherwise. (*a*), (*d*) and (*g*) Graphs computed with tuning widths $s_n=0.15$ (dashed line), 0.25 (solid line) and 0.35 (dotted line). (*b*), (*e*) and (*h*) Graphs computed with baselines $b=5$ (dashed line), 10 (solid line) and 15 (dotted line) Hz. (*c*), (*f*) and (*i*) Graphs computed with response modulations $m=20$ (dashed line), 60 (solid line) and 100 (dotted line) Hz. Changes in response modulation, baseline and tuning width all influence the imaging signal. However, when neurons are tuned to more stimulus dimensions, a smaller proportion of neurons will be driven at high rates by any given stimulus. Therefore, small changes in baseline firing (*h*) can have a much greater impact than large changes in response modulation (*g*) or tuning width (*i*) on population activity (proportional to the area under the curve).

$$p(r|x) = b + m\mathrm{e}^{-(x-x_s^2)/2s_n^2}. \quad (3)$$

Similarly, the probability that any neuron sampled at random from the population has a stimulus of preference x is a multivariate Gaussian with standard deviation s_p (figure 2*b*). This term describes the distribution of neuronal preferences in the population that contributes to the imaging signal,

$$p(x) = \mathrm{e}^{-(x-x_p^2)/2s_p^2}. \quad (4)$$

Equation (4) embodies the topography of functional specialization of any neuronal population, as stimulus preferences are less likely to be found in a given voxel if they depart substantially from the voxel's central preference x_p. From the point of view of our enquiry, the critical determinant of responses is the tuning width of single neurons relative to the population. Therefore, we assume that s_p is unity so s_n becomes the ratio of single neuron tuning width to the range of neuronal preferences within the voxel.

In neuroimaging, the maximal responses in an area are generally considered. One can therefore assume that, in these voxels, x_s and x_p are the same. This lets us reformulate equations (2)–(4) in terms of D, the distance between a neuron's stimulus preference in feature space and the voxel's central stimulus preference where $D = |x - x_p| = |x - x_s|$. Under these assumptions,

$$p(r) = \int_D p(r|D)p(D)\mathrm{d}D \quad (5)$$

where $p(r|D) = b + m\mathrm{e}^{-D^2/2s_n^2}$, $p(D) = (S_d D^{d-1}/2)\mathrm{e}^{-D^2/2s_p^2}$ and S_d is the surface area of a unit sphere in a d-dimensional space.

The results of our model do not depend on the precise nature of the neuronal tuning curve, nor on the precise distribution of preferences within the voxel. We have explored other plausible non-Gaussian tuning curves and distributions of neuronal preference, with very similar results.

(d) *Results of the activation model*

Changes in single neuron tuning width, response modulation and baseline firing all influenced activity in the voxel in a way that depended on the number of stimulus dimensions to which neurons were tuned (figure 3). Changes in response modulation and tuning width mainly influence the signal from neurons whose preferences lie close to the presented stimulus. Changes in baseline firing affect all neurons, including neurons with preferences a long way from the presented stimulus. When neurons are tuned to more stimulus dimensions, simple geometrical considerations reduce the proportion of neurons whose preference lies close to the presented stimulus. This reduces the impact of response modulation and tuning width but greatly amplifies the impact of baseline on imaging signal.

Figure 4 shows how the total population activity A varies with baseline, response modulation, tuning width and the number of stimulus dimensions to which neurons are tuned. First, in line with the MT example (figure 1), simultaneous changes in

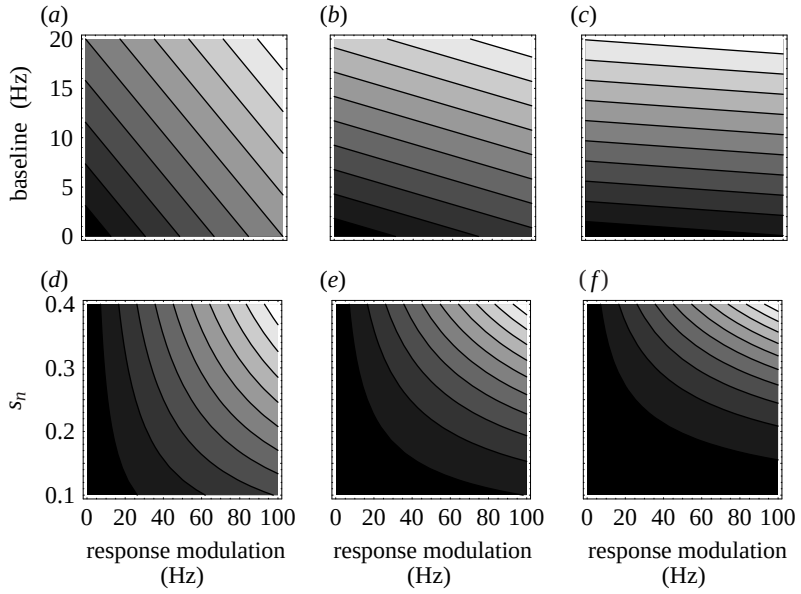

Figure 4. (*a*) $d = 1$, (*b*) $d = 2$, (*c*) $d = 3$, (*d*) $d = 1$, (*e*) $d = 2$, (*f*) $d = 3$. Activation (A) varies with baseline activity, response modulation, tuning and the number of dimensions to which neurons are tuned. The level of activation A is shown by the grey scale, with lighter shades indicating higher activation. Parameters m and b are expressed in units of the mean firing rate and cover physiological ranges. Figure 4*a–c* shows the effects of varying response modulation, m, and baseline firing, b, on population activation, A, when neurons are tuned to (*a*) one, (*b*) two and (*c*) three dimensions. The tuning width was $s_n = 0.25$. Response modulation and baseline changes have additive effects on population activation, so simultaneous shifts in these parameters can make functional changes 'invisible'. However, when neurons are tuned to several stimulus dimensions (*c*) small baseline shifts may outweigh large changes in response modulation. Figure 4*d–f* shows the effects of varying response modulation, m, and tuning width, s_n, on population activation, A, when neurons are tuned to (*d*) one, (*e*) two and (*f*) three dimensions. Changes in the ratio of the tuning width to the range of preferences in the voxel can have a marked effect on population activation. Figure shows 'isoactivity contours', regions where different combinations of tuning width, baseline and response modulation produce identical activity levels.

different tuning parameters may balance out, giving no net change in population activity despite marked changes in information processing. This is shown by the 'isoactivity contours' in figure 4, where different combinations of tuning parameters give identical activation levels. Second, changes in response modulation, the component of neuronal activity often thought to convey the most stimulus-related information, are likely to be hard to detect if neurons are tuned to several stimulus dimensions and/or neuronal tuning is narrow. Third, changes in baseline firing are likely to be highly detectable, particularly when neurons are tuned to several stimulus dimensions. Fourth, changes in tuning width can have a major impact on population activity, particularly when neurons are tuned to several stimulus dimensions.

3. DISCUSSION

Consideration of data from cortical area MT and evidence from our model suggests that population activation cannot distinguish between contributions from response modulation, tuning width, baseline firing and stimulus. Simultaneous changes in these variables can render functional changes 'invisible'. Baseline shifts are likely to be highly detectable relative to changes in response modulation, particularly when neurons are tuned to several stimulus dimensions. If the widely held assumption that imaging signals are closely related to the massed activity of the population of neurons within the voxel is true (Boynton *et al.* 1996; Tagamets & Horwitz 1998), then these results have important implications.

First, it is possible that many functional imaging signals are dominated by changes in attention and not directly by changes in task or stimulus, even in experiments that are not primarily concerned with attention. Psychophysical data show that attentional resolution is orders of magnitude coarser than the corresponding sensory resolution (He *et al.* 1997). Electrophysiology shows that the neurons' attentional modulation is far less selective than the neurons' sensory tuning (Motter 1993; Luck *et al.* 1997). We suppose that this arrangement prevents the attentional filter from setting too strict criteria for stimuli whose precise characteristics are uncertain before their arrival. If the neurons' attentional tuning is indeed broader than their sensory tuning, attentional changes will influence the baseline firing of relatively many cells, but the response modulation of relatively few cells. This may explain why attention is a limited resource and why attentional changes can produce strong signals in functional imaging experiments (e.g. Corbetta *et al.* 1991; Woldorff *et al.* 1997). In addition, as Luck *et al.* (1997) pointed out, stimulus-dependent activation is often transitory, lasting a couple of hundred milliseconds, while attention can increase baseline and response modulation for long periods. Such sustained changes will be even more important than our model suggests when measures of population activation have a temporal resolution longer than the transitory stimulus-driven component of the neuronal response. This is probably the case in human functional imaging where acquisition times are typically several seconds. Therefore, it is particularly important for functional imaging experiments to recognize and explicitly control for factors that

modulate baseline firing, such as attention (and possibly arousal and cognitive load).

Second, learning is accompanied by a reduction in signal in functional imaging (Raichle *et al.* 1994; Jueptner *et al.* 1997) and by increased sparsity in the neural code (Miyashita 1988; Sakai & Miyashita 1991). Since increasing the tightness of tuning reduces the total population activation (figure 3), the decline in neuroimaging signal with learning may reflect learning-dependent improvements in neural coding efficiency (Foldiak 1990; Barlow 1994). Unfamiliar tasks or stimuli may evoke more easily detectable functional imaging signals.

Third, population activation measures are more likely to detect stimulus-driven responses and changes in response modulation by using high-resolution methods to focus on small volumes in which neurons have very similar tuning properties and by exploiting stimulus dimensions that are mapped locally across the cortical sheet. This reduces the effective tuning width and dimensionality of the local neuronal representation. Differential intrinsic optical signals, for example, can resolve cortical columns in which many neurons are simultaneously activated by a single stimulus (Malonek & Grinvald 1996), thus effectively sampling from the most active components of the population distribution.

Fourth, parametric imaging experiments are much less likely to miss functional changes than simple 'cognitive subtractions' (Friston *et al.* 1996). For example, a parametric experiment is unlikely to obtain responses that all run along an 'isoactivation contour' (figure 4; see Friston 1997). At present, however, even factorial designs cannot completely overcome the interactions between tuning width, baseline firing and response modulation because these parameters cannot be manipulated independently. Stimulus characteristics may simultaneously influence response modulation, tuning width or baseline firing (Albright 1984; Britten *et al.* 1992). Attention may simultaneously influence response modulation, neuronal preference, tuning width or baseline firing (Maunsell & Ferrera 1995; Treue & Maunsell 1996; Luck *et al.* 1997). Learning may also simultaneously shift neuronal preference, tuning width and response modulation (Miyashita 1988; Sakai & Miyashita 1991; Fahy *et al.* 1993; Sobotka & Ringo 1993). Hence, the possible ambiguities we identify may be minimized by good design in imaging experiments, particularly by careful control of attention, but cannot at present be resolved entirely.

Our results suggest that functional imaging may focus on the many neurons whose firing rates vary a little since changes in these cells cause the largest changes in population activation. In contrast, conventional single unit electrophysiology has focused on the few neurons whose firing rates vary greatly. Recently, single unit studies have taken more interest in the functional role of the low firing rates that most neurons have for most of the time (e.g. Baddeley *et al.* 1997; Rolls *et al.* 1997; Gallant *et al.* 1998). For example, Rolls *et al.* (1997) found that most of the information carried about a limited set of visual objects by IT cells is carried by neurons with low firing rates. This is because fast-firing neurons, although capable of transmitting large amounts of stimulus-related information, always constitute a small minority of the total population.

We have developed a simple model, based on single cell tuning curves, that accounts for a wide range of results in functional imaging. The novelty of the model resides in the fact that the relationship between single cell and population activity is not the one that is generally supposed. In some cortical areas, baseline shifts, rather than response modulation, may dominate imaging signals. Whatever the relationship between functional imaging and population activation, imaging in humans currently presents a problem of two unknowns: the relation between the signals and underlying neuronal population dynamics is poorly understood and strikingly little is known of the details of human brain neuroanatomy and neurophysiology (Crick & Jones 1993). It is therefore vital that the relationship between functional neuroimaging and neuronal population dynamics is clarified by animal studies in which established neurophysiological techniques run in parallel with imaging methods (e.g. Logothetis *et al.* 1998).

We are grateful to Bill Newsome for MT data and to Karl Friston, Gary Green, Shigeru Yamane, Bruce Cumming, Roland Baddeley and Frank Sengpiel for helpful comments. This study was supported by the Wellcome Trust.

REFERENCES

Albright, T. D. 1984 Direction and orientation selectivity of neurons in visual area MT of the macaque. *J. Neurophys.* **52**, 1106–1130.

Arieli, A., Shoham, D., Hildesheim, R. & Grinvald, A. 1995 Coherent spatiotemporal patterns of ongoing activity revealed by real-time optical imaging coupled with single-unit recording in the cat visual-cortex. *J. Neurophys.* **73**, 2072–2093.

Arieli, A., Sterkin, A., Grinvald, A. & Aersten, A. 1996 Dynamics of ongoing activity: explanation of the large variability in evoked cortical responses. *Science* **273**, 1868–1871.

Baddeley, R., Abbot, L. F., Booth, M. C. A., Sengpiel, F., Freeman, T., Wakeman, E. A. & Rolls, E. T. 1997 Responses of neurons in primary and inferior temporal visual cortices to natural scenes. *Proc. R. Soc. Lond.* B **264,** 1775–1783.

Barlow, H. B. 1994 What is the computational goal of the neocortex. In *Large scale neuronal theories of the brain* (ed C. Koch & J. L. Davis), pp. 1–22. Cambridge, MA: MIT Press.

Boynton, G. M., Engel, S. A., Glover, G. H. & Heeger, D. J. 1996 Linear systems analysis of functional magnetic resonance imaging in human V1. *J. Neurosci.* **16**, 4207–4221.

Britten, K. H., Shadlen, M. N., Newsome, W. T. & Movshon, J. A. 1992 The analysis of visual-motion—a comparison of neuronal and psychophysical performance. *J. Neurosci.* **12**, 4745–4765.

Connor, C. E., Preddie, D. C., Gallant, J. L. & Van Essen, D. C. 1997 Spatial attention effects in macaque area V4. *J. Neurosci.* **17**, 3201–3214.

Corbetta, M., Miezin, F., Dobmeyer, S., Shulman, G. & Petersen, S. 1991 Selective and divided attention during visual discriminations of shape, color, and speed: functional anatomy by positron emission tomography. *J. Neurosci.* **11**, 2363–2402.

Crick, F. H. & Asanuma, C. 1986 Certain aspects of the anatomy and physiology of the cerebral cortex. In *Parallel distributed processing*, vol. 2 (ed. D. E. Rumelhart & J. L. McClelland), pp. 333–371. Cambridge, MA: MIT Press.

Crick, F. J. E. & Jones, E. G. 1993 Backwardness of human neuroanatomy. *Nature* **361**, 109–110.

Douglas, R. J., Koch, C., Mahowald, M., Martin, K. A. C. & Suarez, H. H. 1995 Recurrent excitation in neocortical circuits. *Science* **269**, 981–985.

Engel, S. A., Glover, G. H. & Wandell, B. A. 1997 Retinotopic organization in human visual cortex and the spatial precision of functional MRI. *Cerebr. Cortex* **7**, 181–192.

Fahy, F. L., Riches, I. P. & Brown, M. W. 1993 Neuronal activity related to visual recognition memory: long-term memory and the encoding of recency and familiarity information in the primate anterior and medial inferior temporal and rhinal cortex. *Exp. Brain. Res.* **96**, 457–472.

Foldiak, P. 1990 Forming sparse representations by local anti-Hebbian learning. *Biol. Cybern.* **64**, 165–170.

Friston, K. J. 1997 Imaging cognitive neuroanatomy. *Trends Cognit. Sci.* **1**, 21–27.

Friston, K. J., Price, C. J., Fletcher, P., Moore, C., Frackowiak, R. S. J. & Dolan, R. J. 1996 The trouble with cognitive subtraction. *NeuroImage* **4**, 97–104.

Frith, C. D. & Friston, K. J. 1997 Studying brain function with neuroimaging. In *Cognitive neuroscience* (ed. M. D. Rugg), pp. 169–195. Sussex: Psychology Press.

Gallant, J. L., Connor, C. E. & Van Essen, D. C. 1998 Neural activity in areas V1, V2, and V4 during free viewing of natural scenes compared to controlled viewing. *NeuroReport* **9**, 85–90.

Georgopoulos, A. P., Schwartz, A. B. & Kettner, R. E. 1986 Neuronal population coding of movement direction. *Science* **233**, 1416–1419.

Grinvald, A., Lieke, E. E., Frostig, R. D. & Hildesheim, R. 1994 Cortical point spread function and long-range lateral interactions revealed by real time optical imaging of macaque monkey primary visual cortex. *J. Neurosci.* **14**, 2545–2468.

He, S., Cavanagh, P. & Intriligator, J. 1997 Attentional resolution. *Trends Cogn. Sci.* **1**, 114–120.

Jueptner, M., Stephan, K., Frith, C. D., Brooks, D. J., Frackowiak, R. S. J. & Passingham, R. E. 1997 Anatomy of motor learning. 1. Frontal cortex and attention to action. *J. Neurophys.* **77**, 1313–1324.

Kadekaro, M., Vance, W. H., Terrell, M. L., Gary, H., Eisenberg, H. M. & Sokoloff, L. 1987 Effects of antidromic stimulation of the ventral root on glucose utilization in the ventral horn of the spinal cord in the rat. *Proc. Natl Acad. Sci. USA* **84**, 5492–5495.

Knight, B. W. 1972 The relationship between the firing rate of a single neuron and the level of activity in a population of neurons. Experimental evidence for a resonant enhancement in the population response. *J. Gen. Physiol.* **59**, 767–778.

Kristan, W. B. & Shaw, B. K. 1997 Population coding and behavioural choice. *Curr. Opin. Neurobiol.* **7**, 826–831.

Logothetis, N. K., Peled, S. & Pauls, J. 1998 Development and application of fMRI for visual studies in monkeys. *Soc. Neurosci. Abs.* **24**, 10.11.

Luck, S. J., Chelazzi, L., Hillyard, S. A. & Desimone, R. 1997 Neural mechanisms of spatial selective attention in areas V1, V2, and V4 of macaque visual cortex. *J. Neurophys.* **77**, 24–42.

Malonek, D. & Grinvald, A. 1996 Interactions between electrical activity and cortical microcirculation revealed by imaging spectroscopy: implications for functional brain mapping. *Science* **272**, 551–554.

Maunsell, J. R. & Ferrera, V. P. 1995 Attentional mechanisms in visual cortex. In *The cognitive neurosciences* (ed. M. S. Gazzaniga), pp. 451–461. Cambridge, MA: MIT Press.

Miyashita, Y. 1988 Neuronal correlate of visual associative long-term memory in the primate temporal cortex. *Nature* **335**, 817–820.

Motter, B. C. 1993 Focal attention produces spatially selective processing in visual cortical areas V1, V2, and V4 in the presence of competing stimuli. *J. Neurophys.* **70**, 909–919.

Motter, B. C. 1994 Neural correlates of attentive selection for color and luminance in extrastriate area V4. *J. Neurosci.* **14**, 2178–2189.

Newsome, W. T., Britten, K. H. & Movshon, J. A. 1989 Neuronal correlates of a perceptual decision. *Nature* **341**, 52–54.

Peters, A., Payne, B. R. & Budd, J. 1994 A numerical-analysis of the geniculocortical input to striate cortex in the monkey. *Cerebr. Cortex* **3**, 215–229.

Petersen, S. E., Fox, P. T., Posner, M. I., Mintun, M. & Raichle, M. E. 1988 Positron emission tomographic studies of the cortical anatomy of single word processing. *Nature* **331**, 585–589.

Poeppel, D. 1996 A critical review of PET studies of phonological processing. *Brain Lang.* **55**, 317–351.

Poirson, A., Baseler, H. & Wandell, B. 1997 Color tuning to moving stimuli in the human visual cortex measured using FMRI. *Soc. Neurosci. Abs.* **23**, 550.5.

Raichle, M. E. 1998 Behind the scenes of functional brain imaging: a historical and physiological perspective. *Proc. Natl Acad. Sci. USA* **95**, 765–772.

Raichle, M. E., Fiez, J. A., Videen, T. O., MacLeod, A. K., Pardo, J. V., Fox, P. T. & Petersen, S. E. 1994 Practice related changes in human brain functional anatomy during non-motor learning. *Cerebr. Cortex* **4**, 8–26.

Rolls, E. T., Treves, A., Tovee, M. J. & Panzeri, S. 1997 Information in the neuronal representation of individual stimuli in the primate temporal visual cortex. *J. Comput. Neurosci.* **4**, 309–333.

Sakai, Y. & Miyashita, Y. 1991 Neural organization for the long-term memory of paired associates. *Nature* **354**, 152–155.

Shadlen, M. N. & Newsome, W. T. 1998 The variable discharge of cortical neurons: implications for connectivity, computation, and information coding. *J. Neurosci.* **18**, 3870–3896.

Sobotka, S. & Ringo, J. 1993 Investigation of long term recognition and association memory in unit responses from inferotemporal cortex. *Exp. Brain Res.* **96**, 28–30.

Somers, D. C., Nelson, S. B. & Sur, M. 1995 An emergent model of orientation selectivity in cat visual cortical simple cells. *J. Neurosci.* **15**, 5448–5465.

Tagamets, M. A. & Horwitz, B. 1998 Integrating electrophysiological and anatomical experimental data to create a large-scale model that simulates a delayed match-to-sample human brain imaging study. *Cerebr. Cortex* **8**, 310–320.

Tootell, R. B. H., Reppas, J. B., Kwong, K. K., Malach, R., Born, R. T., Brady, T. J., Rosen, B. R. & Belliveau, J. W. 1995 Functional analysis of human MT and related visual cortical areas using magnetic resonance imaging. *J. Neurosci.* **15**, 3215–3230.

Treue, S. & Maunsell, J. H. R. 1996 Attentional modulation of visual motion processing in cortical areas MT and MST. *Nature* **382**, 539–541.

Van Vreeswijk, C. & Sompolinsky, H. 1998 Chaotic balanced state in a model of cortical circuits. *Neural Comput.* **10**, 1321–1371.

Woldorff, M. G., Fox, P. T., Matzke, P. T., Lancaster, J. L., Veeraswamy, S., Zamarripa, F., Seabolt, M., Glass, J. H., Gao, J. H., Martin, C. C. & Jerabek, P. 1997 Retinotopic organization of early visual spatial attention effects revealed by PET and fMRI. *Hum. Brain Mapp.* **5**, 280–286.

Yarowsky, P., Kadekaro, M. & Sokoloff, L. 1983 Frequency-dependent activation of glucose utilization in the superior cervical ganglion by electrical stimulation of cervical sympathetic trunk. *Proc. Natl Acad. Sci. USA* **80**, 4179–4183.

Zeki, S. M. 1974 Functional organization of a visual area in the posterior bank of the superior temporal sulcus of the rhesus monkey. *J. Physiol.* (*Lond.*) **236**, 549–573.

As this paper exceeds the maximum length normally permitted, the authors have agreed to contribute to production costs.